Biochemical and Biophysical Research Communications 450 (2014) 929–935

Contents lists available at ScienceDirect

Biochemical and Biophysical Research Communications

journal homepage: www.elsevier.com/locate/ybbrc

Atomic resolution structure of the *E. coli* YajR transporter YAM domain

Daohua Jiang [a,b,1], Yan Zhao [a,c,1], Junping Fan [a], Xuehui Liu [a], Yan Wu [a], Wei Feng [a], Xuejun C. Zhang [a,*]

[a] National Laboratory of Macromolecules, National Center of Protein Science-Beijing, Institute of Biophysics, Chinese Academy of Sciences, 15 Datun Road, Beijing 100101, China
[b] School of Life Science and Technology, Huazhong University of Science and Technology, Wuhan, Hubei 430074, China
[c] School of Life Sciences, University of Science and Technology of China, Hefei, Anhui 230027, China

ARTICLE INFO

Article history:
Received 2 June 2014
Available online 19 June 2014

Keywords:
YajR
MFS
Poly-pentagonal water network
Ferredoxin fold

ABSTRACT

YajR is an *Escherichia coli* transporter that belongs to the major facilitator superfamily. Unlike most MFS transporters, YajR contains a carboxyl terminal, cytosolic domain of 67 amino acid residues termed YAM domain. Although it is speculated that the function of this small soluble domain is to regulate the conformational change of the 12-helix transmembrane domain, its precise regulatory role remains unclear. Here, we report the crystal structure of the YAM domain at 1.07-Å resolution, along with its structure determined using nuclear magnetic resonance. Detailed analysis of the high resolution structure revealed a symmetrical dimer in which a belt of well-ordered poly-pentagonal water molecules is embedded. A mutagenesis experiment and a thermal stability assay were used to analyze the putative role of this dimerization in response to changes in halogen concentration.

1. Introduction

The *Escherichia coli* transporter YajR (ecYajR) is a member of the major facilitator superfamily (MFS) of secondary active transporters [1]. Despite initial efforts to elucidate its physiological function, the precise nature of its substrate remains a mystery. Recently, we have reported the crystal structure of the full-length ecYajR, and used it to illustrate the functional roles of its signature motif (motif A) found in most MFS transporters [2]. Apart from the canonical 12-helix transmembrane (TM) domain of the MFS transporter, ecYajR contains a 67-residue, carboxyl-terminal, cytosolic, soluble YAM domain. The naming of YAM reflects the fact that the folding topology and/or sequence homology of this small soluble domain of YajR is similar to that in arabinose efflux permeases (AraEP) as well as in the metal binding domain (MBD) of P-type ATPase transporters. While its functional roles during the transport process remain unknown, the fact that the YAM domain is highly conserved in all known YajR transporters of a variety of Gram-negative bacterial species suggest that its role is essential for the proper functioning of the transporter (Fig. 1A). Importantly, ecYajR exhibits high levels of thermal stability, which is independent of the TM core. Also, the *in vitro* thermal stability of the purified YAM domain increases in response to both increases in pH, and halogen ion concentration (see Fig. S6 in Ref. [2]).

During the determination of the crystal structural of the full-length membrane protein ecYajR which had a medium resolution (3.15 Å), we determined the atomic-resolution crystal structure of the isolated YAM domain at 1.07 Å as well as its nuclear magnetic resonance (NMR) structure. We demonstrate that the YAM domain forms a homodimer in the crystal and possibly in solution as well. The mutation L38A introduced at the dimer interface significantly reduced the thermal stability of the YAM domain, especially at higher concentration of NaCl. These observations suggest that homo-dimerization of the YAM domain may serve as a regulatory mechanism for the full length YajR transporter.

2. Methods

2.1. Protein expression, purification and crystallization

The YAM domain (*i.e.* amino acid residues 388–454 of ecYajR) protein fused with His_6-tag was expressed in the *E. coli* BL21 (DE3). The fusion protein was purified by Ni–NTA affinity chromatography. After removing His6-tag, the protein was further purified by size-exclusion chromatography. The protein samples for NMR were concentrated to ~1.5 mM in 50 mM phosphate buffer (pH 6.3) containing 150 mM NaCl, 1 mM DTT, and 1 mM EDTA.

Crystals of YAM domain were obtained by the hanging drop vapor diffusion method at 16 °C. To get high quality crystals, 1 μl

Abbreviations: MFS, major facilitator superfamily; YAM, YajR/AraEP/MBD domain.

* Corresponding author.
E-mail address: zhangc@ibp.ac.cn (X.C. Zhang).

[1] These authors contribute equally to this project.

http://dx.doi.org/10.1016/j.bbrc.2014.06.053
0006-291X/

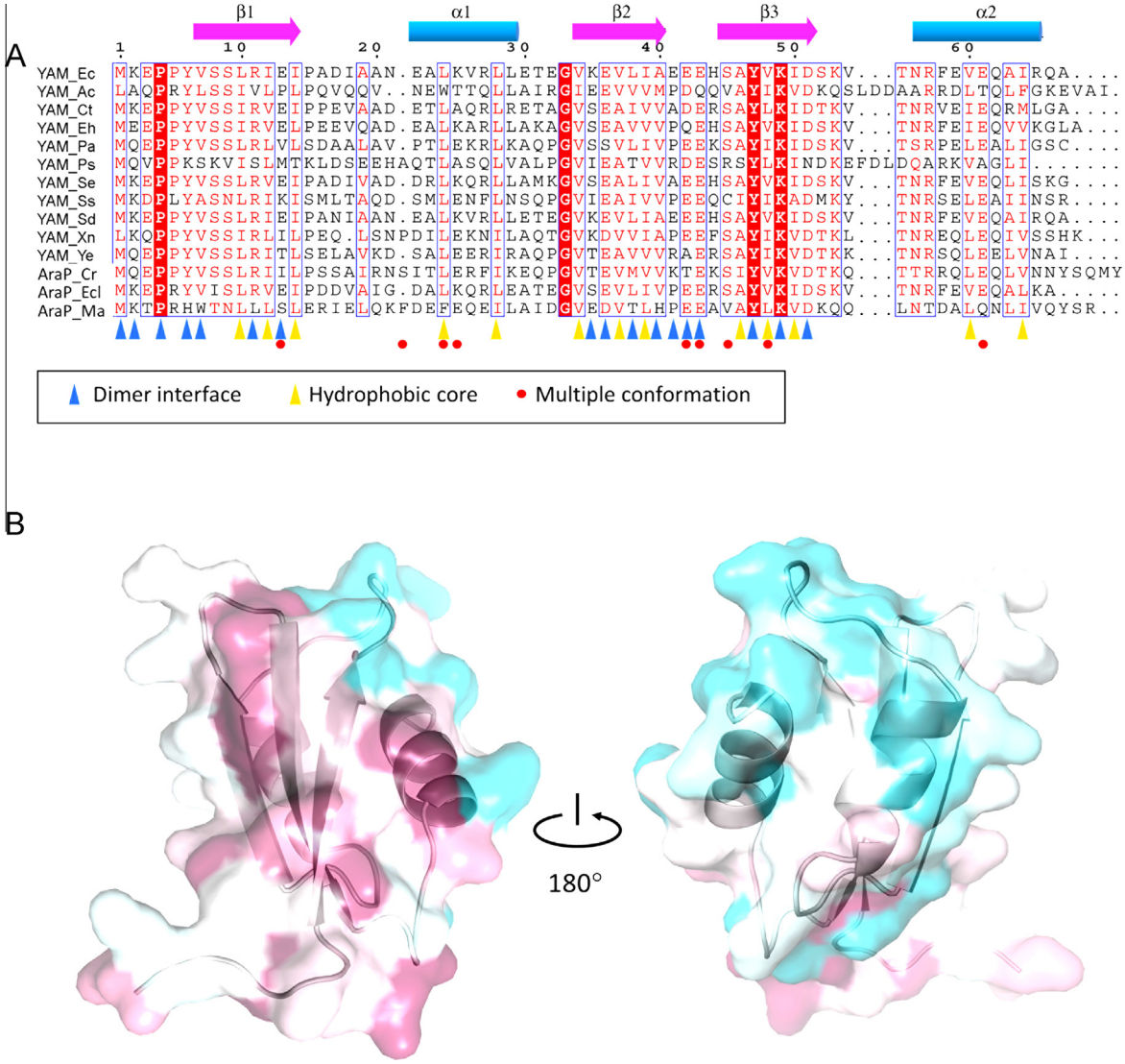

Fig. 1. Conservation of amino acid sequence of the YAM domain. (A) Alignment of amino acid sequences of YajRs from a variety of Gram-negative bacteria. Ec: *E. coli* YajR; Ac: *Acinetobacter calcoaceticus* YajR; Ct: *Cronobac terturicensis* YajR; Eh: *Escherichia hermannii* YajR; Pa: *Pantoea anantis* YajR; Ps: *Pseudoalteromonas* YajR; Se: *Salmonella enteria* YajR; Ss: *Serratia symbiotica* YajR; Sd: *Shigella dysen*teriae YajR; Xn: *Xenorhabdus nematophila* YajR; Ye: *Yersinia enterocolitica* YajR; Cr: *Candidatus Regiellainsecticola* AraP; Ecl: *Enterobacter cloacae* AraP; and Ma: *Methylomicrobium album* AraP. Identical residues are colored in white on red background, similar ones in red on white background. Secondary structural elements of YAM domain from ecYajR are indicated above the sequence alignment. Positions involved in the hydrophobic core are marked with orange triangles at the bottom, those involved in the dimer interface as blue triangles, and those of multiple conformations as red dots. Sequences were aligned with the program *ClustalX* and formatted with *ESPript*. (B) 3D distribution of conserved residues in the YAM domain. The most conserved regions among YajR transporters are in magenta, and the least conserved region in cyan. The 'β-sheet' surface (left) and the hydrophobic core are more conserved than the 'α-helix' surface (right). (For interpretation of the references to color in this figure legend, the reader is referred to the web version of this article.)

concentrated protein of 10 mg/ml was mixed with 1 μl crystallization solution containing 0.1 M HEPES (pH 7.5), 50 mM $CdSO_4$, and 1.0 M sodium acetate. Crystals were cryo-protected with mother liquor supplemented with 20% (v/v) glycerol and flash-cooled in liquid nitrogen. For iodine-derivative, native crystals were soaked in the mother liquor supplemented with 300 mM NaI or KI for 1–2 min.

2.2. Data collection and determination

Diffraction data for the 'native' YAM crystal were collected up to 1.2 Å resolution at the 17U beamline of the Shanghai Synchrotron Radiation Facility (SSRF). The highest resolution data set (up to 1.0 Å) was collected at the 17A beamline of the Photon Factory synchrotron facility (KEK, Japan). Iodine-derivative anomalous data were collected at the 41XU beamline of SPring-8 synchrotron facility (Japan). All data were processed with the program HKL2000 [3].

Initial phases were calculated with the program *Phenix.autosol* [4] using cadmium anomalous signals of the 1.2-Å data. A nearly complete model (Val7–Ala67) was automatically built with *Phenix.autobuild*. After several cycles of geometry-restrained positional and B-factor refinement with *Phenix.refine*, R_{work} dropped to 24.9% (R_{free} 27.1%). Then refinement was carried out using the 1.07 Å resolution data, and R_{work} further dropped to 18.3% (R_{free} 19.7%) after refinement. Model validation was carried out using the *Molprobity* utility [5].

All NMR spectra were acquired at 303 K on an Agilent DD2 600 spectrometer. Backbone and nonaromatic, nonexchangeable side chain resonance assignments of YAM domain were achieved by standard heteronuclear correlation experiments using $^{15}N/^{13}C$-labeled samples and confirmed by a 3D ^{15}N-seperated NOESY

experiment using ^{15}N-labeled samples [6]. Aromatic side chains were assigned by ^{1}H 2D NMR experiment using unlabeled samples in D_2O. Inter-proton distance restraints were derived from 2D ^{1}H-NOESY, 3D ^{15}N-seperated NOESY, and 3D ^{13}C-seperated NOESY spectra. Hydrogen bonding and backbone dihedral angle restraints were generated as described earlier [7]. Structures were calculated using program CNS [8].

2.3. Thermofluor assay

A detailed protocol of the thermofluor analysis was described previously [2]. Briefly, thermofluor analysis performed with a qPCR instrument, Bio-Rad CFX96 (BioRad, US). Sypro Orange dye (Invitrogen, US) was used as the fluorescence probe. The volume of each sample was 20 μl, and the final concentration of the protein was 0.3 μg/μl. The qPCR instrument was programmed to increase temperature from 25 to 95 °C at a rate of 1 °C/min. Melting temperature, Tm, was estimated to be the temperature corresponding to the minimum of the first derivative of the denaturation curve.

3. Results

3.1. Overall crystal structure

The YAM domain of ecYajR consists of 67 a.a residues. It is highly acidic, with a pI value of 4.75. In an earlier report, we performed thermo-denaturation studies on purified recombinant YAM domain [2]. Our results showed that the YAM domain has a melting temperature (Tm) of about 75 °C, and it indicated that its thermal stability increased with rising concentrations of halogen ions, not however, with increasing levels of Na^+/K^+ cations.

The YAM domain was crystallized in the presence of NaCl and $CdSO_4$, at pH 7.5. In the following description of the isolated YAM domain, we refer to the full length ecYajR amino acid residues 388–454 as residue numbers 1–67. In the refined model, three residues from leftover of a thrombin cleavage are labeled as −3 to −1. The crystal of YAM domain diffracted X-ray up to 1.07-Å resolution. The space group is $C222_1$. There is one protein molecule per crystallographic asymmetric unit, with 47% solvent content (V_M = 2.4 Å^3/Da) [9]. The average B factor of the YAM domain is 28.9 Å^2. The overall structure of the YAM domain is similar to that reported for the full length ecYajR crystal structure (Protein Data Bank (PDB) ID: 3WDO) with a root mean square (r.m.s.) deviation of 0.59 Å for 62 Cα-atom pairs. Ten residues were refined with multiple conformations. Statistics of the data collection and refinement of the crystal structure are summarized in Table S1.

As described in the previously published report of the full-length YajR structure [2], the YAM domain possesses a modified version of the so-called ferredoxin fold [10] and has dimensions of 22 × 25 × 37 Å^3 (Fig. 1B). While ferredoxin folds usually have a βαββαβ secondary structure pattern, the last β-strand is missing in the YAM domain. The remaining three β-strands form one anti-parallel β-sheet, with the two α-helices located on one side of the sheet. As shown in Fig. 1B, we refer to the two surfaces of the molecule as β-sheet surface and α-helix surface. In general, the amino acid residues of the β-sheet are more conserved than those in other parts of the protein molecule (Fig. 1B). We therefore predicted that the modified ferredoxin fold of the YAM domain is conserved in all YajR transporters.

3.2. Dimerization

In the crystal packing, there is one twofold symmetrical protein–protein interaction (related by the dyad axis along the crystallographic *a* axis). The interface is located between the β-sheet surfaces from two neighboring YAM molecules. With solvent molecules excluded, this interface buries a total of 1700 Å^2 of solvent accessible surface (SAS), while other crystal packings involve buried interfaces of less than 500 Å^2. According to analysis of protein–protein interfaces of crystal structures present in the Protein Data Bank, such a large protein–protein interface of 1700 Å^2 is likely to be of biological significance [11]. This dimer interface was not identified in the full length YajR crystal structure, instead the formation of trimers was observed. However, in this trimer, the YAM domains only participate in loose packing of the YajR crystal structure. Correspondingly, the average B-factor of the YAM domain was rather high (107 Å^2), which is significantly higher than that of the TM domain (59 Å^2). In the current YAM crystal structure, most of the dimer interface is formed by polar interactions, including inter-molecular salt-bridge bonds, *e.g.* Glu36 (highly conserved as shown in Fig. 1A) – Lys49' (absolutely conserved) and Glu42 (conserved) – Arg11' (conserved), and main-chain carbonyl atoms of both Glu42 and Glu43 with the side chain of Glu43' (conserved). The only hydrophobic interaction in the interface is formed by side chains of Leu38 (conserved as hydrophobic residues) and Tyr47 (absolutely conserved) from the two neighboring protomers. In addition, among YajR transporters from different species, there are only four absolutely conserved residues (Fig. 1A). Three of them are located within the βαββα core, namely Gly33 (which is required for the structure or folding of the protomer), Tyr47, and Lys49. The latter two are located in the dimer interface, and Lys49 participates in the inter-molecular salt-bridge bonds. Therefore, the dimer interface of the YAM domain appears to be conserved among YajR proteins. Together, these data suggest that under certain conditions, the observed dimer in the crystal structure may also exist in solution.

The N-terminal peptides (*i.e.* residues 4–6) of the dyad-symmetry related YAM domains run anti parallel to each other but did not form a β-sheet. Individual superposition of the full-length ecYajR crystal structure to both protomers of the YAM dimer results in structural collision between the TM domain of one molecule and YAM domain of the other. It suggests that the YAM domain observed in the full length ecYajR has to move relative to the TM core of YajR, if a YAM dimer similar to that observed in the current structure is to be formed in the context of full length YajR.

To verify the biological relevance of the dimer, we introduced the point mutation L38A. Thermal stability analysis of the L38A variant showed reduced thermal stability compared to WT, especially at higher concentrations of NaCl (Fig. 2). Since Leu38 would be solvent-exposed in the protomer, the mutation is unlikely to disrupt the overall structure of YAM in its monomeric form. Therefore, we interpret the observed loss of thermal stability of the L38A variant as a result of dissociation of the dimer.

3.3. NMR structure and backbone dynamics of the YAM domain

The YAM domain structure was also studied using an NMR spectroscopic approach. The solution structure of the YAM domain determined by NMR spectroscopy is represented in backbone superposition in Fig. 3A, and the NMR data used for structure calculation are summarized in Table S2. The NMR structure of the YAM domain is similar to that determined by crystal structure analysis. The r.m.s. deviation between the crystal structure and the NMR structure (*i.e.* the model of lowest free energy) is 1.77 Å (for 60 Cα-atom pairs). Structural differences mainly include structural shifts in the N-terminal peptide, the β1-α1 loop, and α2 regions. To investigate whether the solution structure also forms a dimer, we calculated the inter-molecular contact of protons within 5 Å from the potential interface and searched the NOESY spectra for any featured NOEs. No inter-molecular NOE was identified under the experimental condition. To characterize the

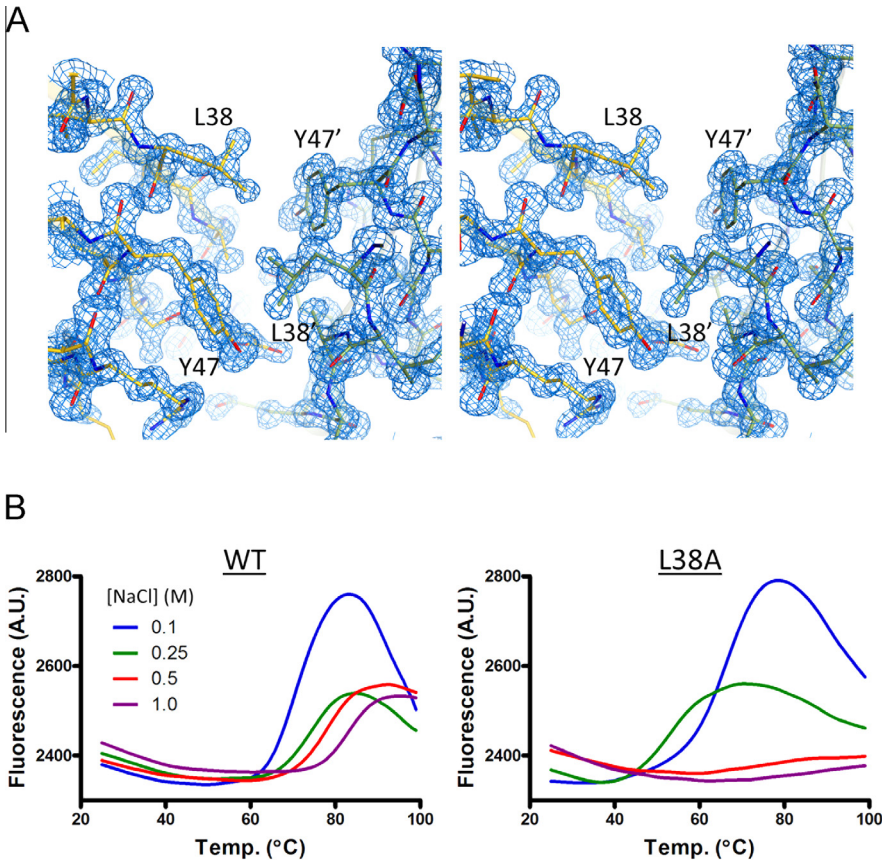

Fig. 2. The effect of L38A mutation on YAM thermal stability. (A) Stereo view of Leu38 in the dimer interface. 2Fo–Fc electron density map was contoured at 2.0 σ. (B) Thermal denature curves of WT YAM (left) and the L38A variant (right). Melting temperatures (Tm) of the WT were 69.5, 73.0, 77.7, and 83.3 °C for [NaCl] of 0.1, 0.25, 0.5, and 1.0 M, respectively. The Tm values of the L38A variant were 62.7 and 52.0 °C for [NaCl] of 0.1 and 0.25 M, respectively, and could not be determined for higher NaCl concentrations.

plasticity of the YAM domain, we measured the backbone relaxation data. Not surprisingly, the heteronuclear NOE showed a uniform value of $0.77 \pm 0.08\ s^{-1}$ (ranging from 0.57 to $0.95\ s^{-1}$), implying that the entire domain is rigid with little internal motion in the pico- to nano-second timescale (Fig. 3B upper panel). The longitudinal relaxation rates were also fairly constant throughout the sequence, with an average value of $1.86 \pm 0.62\ s^{-1}$ (ranging from 1.51 to $2.80\ s^{-1}$) (Fig. 3B lower panel). Only a few residues located within loop regions experienced some degree of internal mobility, as was apparent from the higher R_1 and lower NOE values (Fig. 3B). In contrast, some of the residues showed unexpected higher relaxation rates (middle panel of Fig. 3B), implying the occurrence of conformational exchanges between these residues on a micro- to milli-second timescale. Together, the overall NMR solution structure of the YAM domain appears to be similar to that of the protomer observed in the crystal structure.

3.4. Water networks

In the dimer interface of the crystal structure of YAM, there is a water channel formed between the two β-sheets. Water molecules form a curved poly-pentagonal belt that passes through this channel that contains 8 water rings (Fig. 4). The two end rings are six-membered rings, with an oxygen atom coming from the carboxyl side chain of Glu41, and the rest six fused rings are pentagonal. Similar poly-pentagonal water belts have been studied by inorganic chemists, both theoretically and experimentally [12]. The water belt forms multiple hydrogen bonds with the main-chain polar atoms that are located in a groove of the β-sheet (at Leu10, Val48, and Val37). Extensive poly-pentagonal water networks in protein structures were first observed in the crystal structure of crambin (PDB ID: 1CRN; 0.945-Å resolution), a 46-residue seed storage protein [13]. Recently, poly-pentagonal water networks were reported in the crystal structure of Maxi, a helix-bundle antifreeze protein from winter flounder (*Pseudopleuronectes americanus*) (PDB ID: 4KE2; 1.8 Å) [14]. In Maxi, the poly-pentagonal water networks also interact primarily with the main-chain polar atoms of the peptides.

Since the thermal stability of the YAM domain increases with halogen ion concentration [2], we soaked our crystals with sodium iodide in an attempt to identify halogen binding site(s). Within this iodide-soaked crystal (1.5-Å resolution), we identified 14 sites (>4 σ) of iodide ions in an anomalous difference Fourier map. All of these sites occupied positions nearly identical to those of some 'water' molecules in the native crystal. In particular, electron density peaks were found at positions near the center of the poly-pentagonal belt (*i.e.* near the crystallography dyad axis) (Fig. 4C). Therefore, it can be assumed that in the native crystal, some of these sites were occupied by chloride ions that originated from the crystallization buffer. Although many iodide sites appeared to be clustered together, they may not be occupied simultaneously. This argument is based on the fact that iodide ions carry negative charges, and ions carrying the same charges would not form close contacts with each other, unless these charges were delocalized. In fact, the occupancies of all iodide ions observed in our refined crystal structure were about 0.5 or lower. Since the poly-pentagonal belt is located at the conserved dimer interface, doping of the water belt with halogen ions may influence the

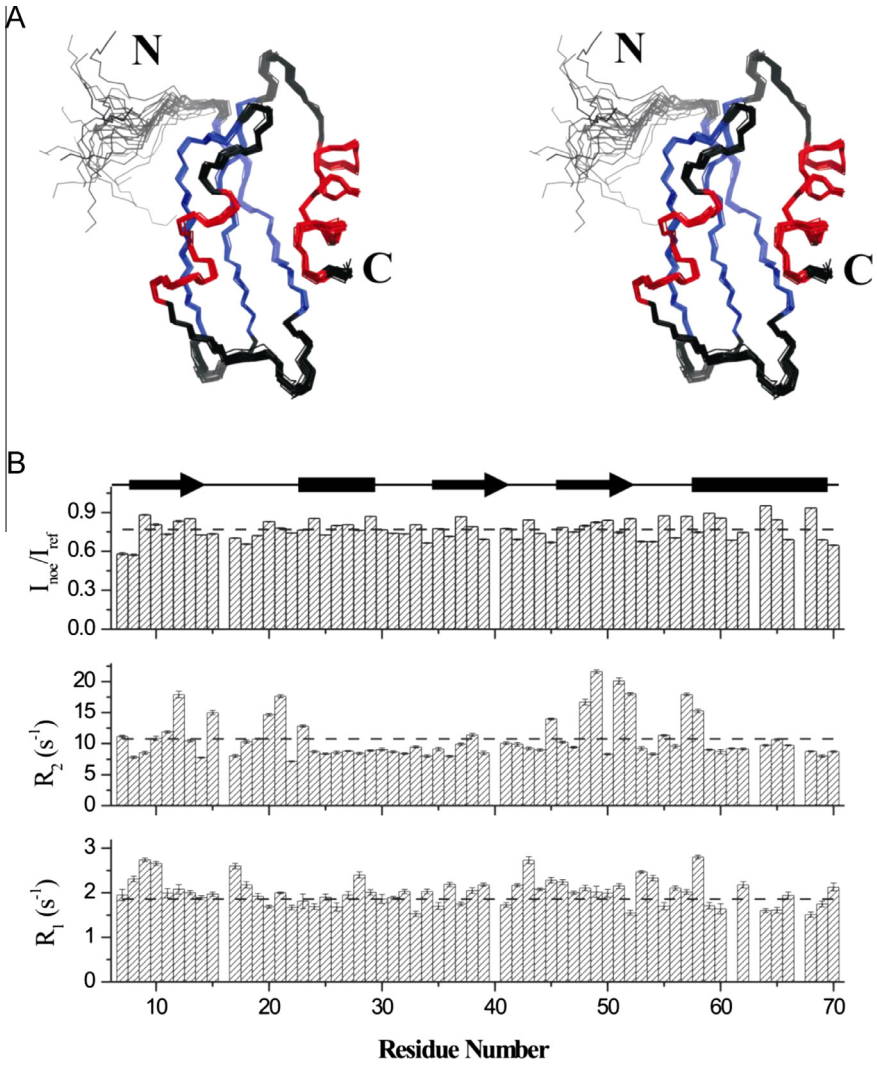

Fig. 3. Solution structure of YAM domain and backbone dynamics data derived from NMR spectroscopy. (A) Stereo view of backbone superposition of the 20 lowest-free energy structures of the YAM domain. Helix regions are shown in red, sheet regions in blue, while other parts are indicated in black. The N- and C-termini is labeled N and C respectively. (B) Backbone dynamics data vs. residue number showing heteronuclear NOE (upper panel), transverse relaxation rate (middle panel) and longitudinal relaxation rate. The dashed line in each panel represents the average value of that specific data. (For interpretation of the references to color in this figure legend, the reader is referred to the web version of this article.)

process of dimerization, thus providing a putative explanation to the effect of halogen concentration on the thermal stability of the YAM domain [2]. Compared to WT, the L38A mutation showed the opposite effect of halogen ions on protein stability (Fig. 2B). One possible explanation would be that the dimerization, and therefore the formation of the water belt, did not occur in this mutant.

3.5. Homologous structures

As mentioned above, the folding topology of the YAM domain is similar to that of the N-terminal MBD domain of P1-type ATPase, a heavy metal transporter (PDB ID: 3DXS; 1.7 Å) [10]. Although it is postulated that this MBD domain regulates the transport of its substrates (*e.g.* metal cations), the precise details of the regulatory mechanisms involved are currently unclear. The crystal structure of the MBD domain can be superimposed to YAM with a 0.79 Å rmsd (for 56 Cα-atom pairs) (Fig. S1), which is surprisingly small for a pair of proteins that share a rather low sequence homology (12% identity, 25% consensus). The canonical βαββαβ sequence of secondary elements in ferredoxin-like domains forms a hairpin ribbon (*i.e.* βαβ x2) before it folds further into a right-hand helical structure, in which the four β-strands form an antiparallel β-sheet. Therefore, this type of domain may exhibit a simple folding dynamics, and therefore be evolutionarily favored to perform a variety of simple functions such as binding ions. The hydrophobic core is conserved and very important for the stability of this βαβϖ βαβ folding, and a single point mutation in this core may result in unfolding of the domain [15]. Moreover, the MBD domain does not form a symmetrical dimer in its crystal structure. The copper binding site of the MBD, located in the region between β1 and α1, is not conserved in the YAM domain of YajR. In contrast, there is one fully occupied cadmium site in the YAM crystal (Fig. S1), which was used to determine the initial phases of the crystal structure. In particular, a cadmium cation (with an occupancy of 1.0 and a B-factor of 18.3 $Å^2$) binds to the side chain of His44 in the loop between β2 and β3. Thus, although the YAM domain of YajR shares the same folding topology with the MBD domain of P1-type ATPase, they may be involved in different regulatory mechanisms.

3.6. Possible regulation mechanism

The YAM domain is conserved in all known YajR transporters of Gram-negative bacteria. As an MFS transporter, YajR contains two

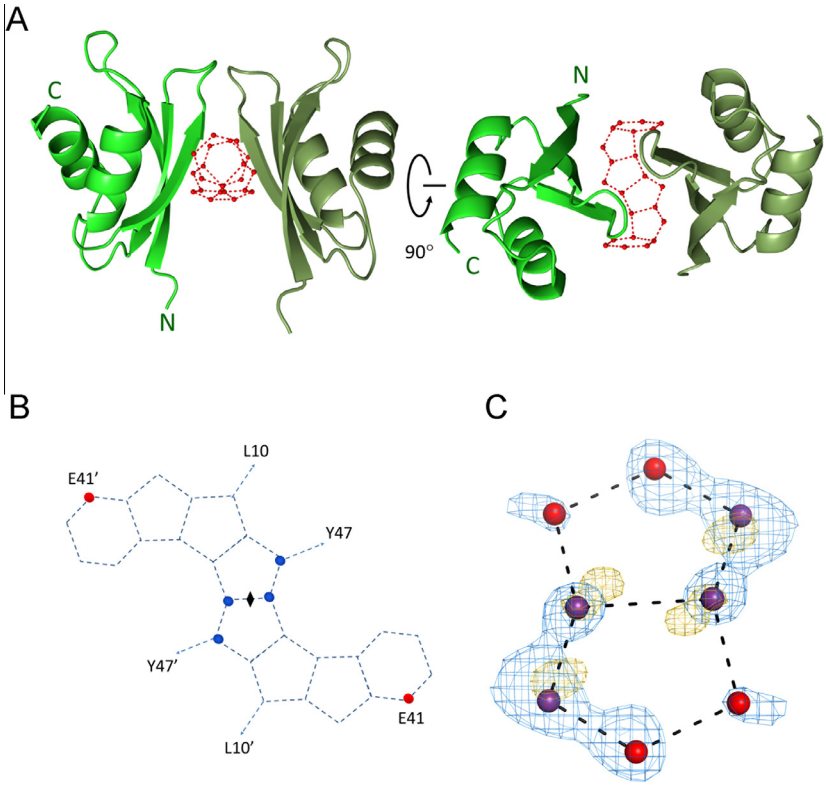

Fig. 4. Poly-pentagonal water rings observed in the crystal structure. (A) Ribbon representation of the symmetrical dimer of the YAM domain. The belt of poly-pentagonal water rings is included. (B) Schematic diagram of the poly-pentagonal 'water' belt. The dyad axis is depicted as a diamond, iodide ion-doped positions as blue dots, and polar atoms from Glu41 as red dots. Neighboring residues that contribute backbone carbonyl oxygen atoms to form hydrogen bonds with the water belt are labeled. (C) Iodide ions doped into the water rings. 2Fo–Fc map of the native crystal is contoured at 1.0 σ and colored in blue. Anomalous differential Fourier map of the iodide soaked crystal is contoured at 3.0 σ and colored in gold. Solvent molecules from the refined crystal structure are superimposed, with iodine in purple and water in red. (For interpretation of the references to color in this figure legend, the reader is referred to the web version of this article.)

TM domains (N- and C-domains), each consisting of six TM helices [2]. These two domains are related to each other by a pseudo-dyad symmetry. The relative movements of the two domains result in two major conformations, namely inward-facing and outward-facing, allowing the substrate to be transported across the membrane. The degree of conservation of the YAM domain suggests that it has an important regulatory role to play in YajR transporter function, though the precise nature of the YajR substrate remains to be determined. One possible mechanism of how the YAM domain might regulate YajR transport can be proposed as follows: In the ecYajR structure, the cytosolic YAM domain and the TM core are linked by a flexible loop (*i.e.* residues 388–393 of ecYajR). The C-domain of YajR contains a so-called A-like motif in a loop between TM helices 8 and 9 (referred to as motif A^{L8-9}), which contains a signature acidic residue (*i.e.* Glu272 in ecYajR) [2]. The main function of this motif is postulated to be the stabilization of the outward conformation through an inter-domain, charge-dipole interaction between the acidic residue of motif A^{L8-9} and the N-terminal end of TM5, as observed in the YajR crystal structure. Because of its electrostatic nature, this interaction is sensitive to change of the electrostatic field. The YAM domain is highly negatively charged (pI: 4.75). Therefore, when the YAM domain is in close proximity to the TM C-domain, it may stabilize the inter-domain interaction associated with motif A^{L8-9}. Dimerization of the YAM domain would then pull the YAM domain away from the TM C-domain, thus reducing the stability of the outward conformation of YajR. Therefore, by manipulating dimerization of the YAM domain (*e.g.* in response to changes of halogen concentration), the transport activity of YajR can be regulated through the interaction between the YAM domain and motif-A^{L8-9}. Interestingly, three YajR transporters from Gram-positive bacteria (*Betaproteobacteria bacterium*, *Buchnera aphidicola*, and *Wigglesworthia glossinidia*) that do not possess a YAM domain also lack the motif A^{L8-9}, suggesting a functional relationship between the two. Identifying the actual substrate for YajR would constitute a major step towards verifying this hypothesis.

4. Protein Data Bank accession number

The diffraction data and refined coordinates of the crystal structures of YAM domain have been deposited into PDB. The accession codes are 4Q2L for the native crystal and 4Q2M for the iodine soaked one, respectively. Those of the NMR structures of the YAM domain have also been deposited. The accession code is 2RU9.

Acknowledgments

The authors thank the staff of the Protein Research Core Facility at the Institute of Biophysics, Chinese Academy of Sciences (CAS), for their excellent technical support. We are grateful to staff members of SSRF (China), SPring-8 (Japan), and Photon Factory (Japan) synchrotron facilities for their assistance in data collection. This work was supported by the Ministry of Science and Technology (China) (Grant 2011CB910301 to XCZ).

Appendix A. Supplementary data

Supplementary data associated with this article can be found, in the online version, at http://dx.doi.org/10.1016/j.bbrc.2014.06.053.

References

[1] K. Nishino, A. Yamaguchi, Analysis of a complete library of putative drug transporter genes in *Escherichia coli*, J. Bacteriol. 183 (2001) 5803–5812.

[2] D. Jiang, Y. Zhao, X. Wang, J. Fan, J. Heng, X. Liu, W. Feng, X. Kang, B. Huang, J. Liu, X.C. Zhang, Structure of the YajR transporter suggests a transport mechanism based on the conserved motif A, Proc. Natl. Acad. Sci. U.S.A. 110 (2013) 14664–14669.

[3] Z. Otwinowski, W. Minor, Processing of X-ray diffraction data collected in oscillation mode, Methods Enzymol. 276 (1997) 307–326.

[4] P.D. Adams, P.V. Afonine, G. Bunkoczi, V.B. Chen, I.W. Davis, N. Echols, J.J. Headd, L.W. Hung, G.J. Kapral, R.W. Grosse-Kunstleve, A.J. McCoy, N.W. Moriarty, R. Oeffner, R.J. Read, D.C. Richardson, J.S. Richardson, T.C. Terwilliger, P.H. Zwart, PHENIX: a comprehensive Python-based system for macromolecular structure solution, Acta Crystallogr. D Biol. Crystallogr. 66 (2010) 213–221.

[5] I.W. Davis, L.W. Murray, J.S. Richardson, D.C. Richardson, MOLPROBITY: structure validation and all-atom contact analysis for nucleic acids and their complexes, Nucleic Acids Res. 32 (2004) W615–W619.

[6] L.E. Kay, K.H. Gardner, Solution NMR spectroscopy beyond 25 kDa, Curr. Opin. Struct. Biol. 7 (1997) 722–731.

[7] W. Feng, J.F. Long, J.S. Fan, T. Suetake, M. Zhang, The tetrameric L27 domain complex as an organization platform for supramolecular assemblies, Nat. Struct. Mol. Biol. 11 (2004) 475–480.

[8] A.T. Brunger, P.D. Adams, G.M. Clore, W.L. DeLano, P. Gros, R.W. Grosse-Kunstleve, J.S. Jiang, J. Kuszewski, M. Nilges, N.S. Pannu, R.J. Read, L.M. Rice, T. Simonson, G.L. Warren, Crystallography & NMR system: a new software suite for macromolecular structure determination, Acta Crystallogr. D Biol. Crystallogr. 54 (1998) 905–921.

[9] B.W. Matthews, Solvent contents of protein crystals, J. Mol. Biol. 33 (1968) 491–497.

[10] M. Zimmermann, O. Clarke, J.M. Gulbis, D.W. Keizer, R.S. Jarvis, C.S. Cobbett, M.G. Hinds, Z. Xiao, A.G. Wedd, Metal binding affinities of Arabidopsis zinc and copper transporters: selectivities match the relative, but not the absolute, affinities of their amino-terminal domains, Biochemistry 48 (2009) 11640–11654.

[11] L. Lo Conte, C. Chothia, J. Janin, The atomic structure of protein–protein recognition sites, J. Mol. Biol. 285 (1999) 2177–2198.

[12] B.Q. Ma, H.L. Sun, S. Gao, Cyclic water pentamer in a tape-like structure, Chem. Commun. (2004) 2220–2221.

[13] M.M. Teeter, Water structure of a hydrophobic protein at atomic resolution: Pentagon rings of water molecules in crystals of crambin, Proc. Natl. Acad. Sci. U.S.A. 81 (1984) 6014–6018.

[14] T. Sun, F.H. Lin, R.L. Campbell, J.S. Allingham, P.L. Davies, An antifreeze protein folds with an interior network of more than 400 semi-clathrate waters, Science 343 (2014) 795–798.

[15] L. Banci, I. Bertini, S. Ciofi-Baffoni, L. Gonnelli, X.C. Su, A core mutation affecting the folding properties of a soluble domain of the ATPase protein CopA from Bacillus subtilis, J. Mol. Biol. 331 (2003) 473–484.